

Spherical iron/silica nanocomposites from core-shell particles

Manuel Ocaña^{a,*}, Manuel Andrés-Vergés^b, Raúl Pozas^a, Carlos J. Serna^c

^a *Instituto de Ciencia de Materiales de Sevilla (CSIC-UNSE), Americo Vespucio s/n, Isla de La Cartuja, 41092 Sevilla, Spain*

^b *Departamento de Química Inorgánica, Universidad de Extremadura, Avda. de Elvas s/n, 06071 Badajoz, Spain*

^c *Instituto de Ciencia de Materiales de Madrid (CSIC), Cantoblanco, 28049 Madrid, Spain*

Received 20 April 2005; accepted 13 July 2005

Available online 6 September 2005

Abstract

A simple procedure to coat silica spheres with smooth layers of iron compounds is reported. It is based on the forced hydrolysis (60–85 °C) of iron(III) acetylacetonate solutions containing the silica cores and sodium dodecylsulfate (SDS). The role that the iron(III) precursor and SDS play in the formation of uniform coatings is discussed. The thermal evolution of the composites up to the crystallization of the initially amorphous coating was also studied. Finally, the core-shell particles, as prepared, were thermally reduced under hydrogen atmosphere to produce magnetic composites whose magnetic properties were also evaluated as a function of the reduction temperature.

© 2005 Elsevier Inc. All rights reserved.

Keywords: Core-shell; Coating; Iron; Iron oxide; Silica; Magnetic properties

1. Introduction

Nowadays, there is a growing interest in the preparation of core-shell particles because the properties of these composite solids can be tailored by the appropriate choice of the core and the shell nature, which confer to these systems a wide range of applications [1,2]. One of the most studied systems among these materials are probably those having shells consisting of iron compounds, which have uses in various fields of science and technology. Thus, different iron oxide phases (hematite and magnetite) deposited on silica surfaces have been shown to be useful catalysts for several processes [3,4]. Dispersions of nonmagnetic spheres coated with magnetic iron compounds can be also used in biotechnology for the magnetically-assisted separation of biochemical products and cells [5] and for cancer treatment [6]. Most of these studies have been conducted using polymers as core compounds [7,8]. However, for many of these applications the use of inorganic cores would be advantageous since they give superior thermal stability to the composites which

permits to modulate their magnetic properties by a simple thermal treatment [9]. The most interesting inorganic core is probably amorphous silica (SiO₂), which can be synthesized with tailored size, spherical shape, and narrow size distribution by using the Stöber procedure [10].

Whereas the deposition of uniform silica shells on iron oxide particles has been successfully carried out by different procedures [11,12], the opposite process (iron compounds on silica) is much more difficult. In fact, only a few attempts to deposit iron compounds on silica spheres can be found in literature, which in general did not result in homogeneous coatings. Thus, the sonication of Fe(CO)₅ solutions in decalin, in which the silica cores were previously dispersed resulted in heterogeneous systems consisting of irregular nanoparticles or clusters of partially oxidized/hydrolyzed iron not adhered uniformly to the silica particles [13]. The coating of silica spheres with layers of preformed magnetite (Fe₃O₄) nanoparticles (10 nm) using a heterocoagulation process facilitated by charging the silica surface through the addition of a polyelectrolyte film has been also reported although this method also produced rough coatings [14]. More recently, smooth layers (6 nm) of maghemite (γ-Fe₂O₃) could be deposited on spherical silica particles by a method

* Corresponding author.

E-mail address: mjurado@icmse.csic.es (M. Ocaña).

based on the surface precipitation from iron ammonium citrate solutions assisted by urea decomposition, which also involved the previous alternating adsorption of a cationic and an anionic polyelectrolyte onto the silica surface [9].

In this paper we offer an alternative and simpler procedure to coat silica spheres with smooth layers of iron compounds through the forced hydrolysis (60–85 °C) of iron(III) acetylacetonate ($\text{Fe}(\text{acac})_3$) solutions containing the silica cores and sodium dodecylsulfate (SDS). This procedure yielded amorphous coatings for which the thermal evolution of the composites up to crystallization was also studied. Finally, the so obtained core-shell particles were also thermally reduced under hydrogen atmosphere to produce iron/silica composites whose magnetic properties were evaluated.

2. Experimental

2.1. Chemicals

Ethanol absolute (GR, Merck), tetraethyl orthosilicate (TEOS) (98%, Aldrich), ammonium hydroxide (28%, Fluka), iron(III) chloride hexahydrate (99%, Merck), iron(III) nitrate nonahydrate (98%, Riedel-de Haën), iron(III) acetylacetonate (97%, Fluka), and sodium dodecylsulfate (SDS) (99%, Sigma) were used as received.

2.2. Preparation of the silica cores

The silica cores were synthesized according to the Stöber method [10], by base-catalyzed hydrolysis of TEOS in ethanol solutions at 40 °C, for 1 h. The TEOS, H_2O , and NH_4OH concentrations in these solutions were 0.26, 1.67, and 1.07 mol dm^{-3} , respectively. After aging, the precipitates were washed first with ethanol and then with doubly distilled water, collected by filtration and dried at 50 °C. This procedure resulted in uniform spherical particles having a mean diameter of 510 nm and a standard deviation of 34.

2.3. Coating procedure

In order to establish the optimum conditions to deposit uniform layers of iron compounds on monodispersed silica spheres, we first studied the influence of the nature of the iron precursor (chloride, nitrate, and acetylacetonate) on the coating characteristics. Since the addition of SDS has also been reported to improve the uniformity of the coating in similar systems (Co compounds on silica) [15], some assays were also carried out in the presence of this surfactant. For these experiments, a sonicated aqueous dispersion of SiO_2 cores (1.8 g dm^{-3}) was added to a solution containing the iron(III) precursor (0.002 mol dm^{-3}) and SDS (when used). In the case of $\text{Fe}(\text{acac})_3$, a water/ethanol mixture (volume ratio = 1:1) was used as solvent since the solubility of this iron compound in water is very low. The so prepared

dispersions were then aged under stirring at constant temperature (85 °C) for 24 h in tightly capped Pyrex test tubes after which, the solids obtained were centrifuged and washed with doubly distilled water. This purification procedure was repeated several times to eliminate the excess of electrolyte and SDS. The so purified solids were finally collected by filtration and dried at 50 °C.

The concentration of the iron salts and the amount of SiO_2 cores were systematically varied aiming to control the coating thickness.

For comparison purposes, an iron oxide/SDS blank was also prepared by aging at 85 °C for 24 h $\text{Fe}(\text{acac})_3$ solutions (0.002 mol dm^{-3}) in the presence of SDS (SDS/ $\text{Fe}(\text{acac})_3$ mole ratio = 15).

2.4. Thermal treatments and reduction

The calcination of the samples was carried out by heating the furnace at 10 °C min^{-1} up to the desired temperature at which they were held for 3 h.

The core-shell particles were reduced for 3 h at constant temperature in a hydrogen stream introduced into the reactor at a constant flow rate (2 $\text{dm}^3 \text{h}^{-1}$). The samples were then cooled to room temperature under the hydrogen atmosphere. The reduction temperature was varied between 300 and 400 °C to modulate the magnetic properties of the composites.

2.5. Characterization techniques

Transmission electron microscopy (TEM, Philips 200 CM) was used to examine particle size and shape and the effectiveness of the coating procedure. The particle size distribution of the cores was evaluated from the electron micrographs by counting around one hundred particles.

The quantitative composition of the samples in terms of the Fe/Si atomic ratio was determined by X-ray fluorescence (XRF, Siemens SRS 3000). Infrared spectroscopy (IR) was also used to gain information on samples composition. The IR absorption spectra of the powders diluted in KBr were recorded in a Nicolet 510 FT-IR spectrometer, whereas the diffuse reflectance infrared spectra (DRIFTS) were obtained in a JASCO FT/IR-6300 apparatus. Energy dispersive X-ray analysis (EDX, Philips DX4), installed in the TEM microscope, was also used to assess the homogeneity in composition at the particle level.

Identification of the crystalline phases was carried out by X-ray diffraction (XRD) in a Siemens D501 apparatus using $\text{CuK}\alpha$ radiation and a diffracted beam graphite monochromator.

The isoelectric point (iep) of the samples was determined (Malvern Zetamaster) by measuring electrophoretic mobilities of aqueous dispersions as a function of pH. Between 3 and 5 mg of sample were dispersed in 100 cm^3 of a 0.01 mol dm^{-3} KNO_3 solution to keep the ionic strength constant, while the pH was varied by adding HNO_3 or KOH .

X-Ray photoelectron spectra (XPS) were recorded in a VG Escalab 220 using the MgK_{α} excitation source. Calibration of the binding energy scale of the spectra was done at the C_{1s} peak of the surface carbon contamination taken at 284.6 eV. Atomic percentages of the elements were calculated from the peaks areas after background subtraction (Shirley background). The areas were referred to the sensitivity factors of the elements as supplied by the instrument manufactures.

Magnetic characterization of the samples was carried out in a vibrating sample magnetometer (VSM). The saturation magnetization (M_s), coercivity (H_c), and squareness (M_r/M_s , where M_r is the remanent magnetization) were obtained from the hysteresis loops for each sample recorded at 298 K after applying a saturating field of 3 T. The M_s values were evaluated by extrapolating to infinite field the experimental results obtained in the high field range where the magnetization linearly decreases with $1/H$.

3. Results and discussion

3.1. Preparation and characterization of core-shell particles

The forced hydrolysis at 85 °C of the iron(III) salt (chloride or nitrate) solutions containing the silica cores did not yield coated particles. Instead, mixed systems consisting of silica spheres and irregular particles of the precipitated iron compounds were observed. However, irregularly coated particles with rough surfaces were obtained from $Fe(acac)_3$ solutions, although evidence of some irregular particles of iron compounds was still detected (Figs. 1a and 1b). This different behaviour could be explained by the different pH of the dispersions. Thus, when using the inorganic salts, the pH (2.7 ± 0.1) was lower than the iep of silica (2.9) (Fig. 2) and also than those reported for most iron hydroxides and oxides [16]. Therefore, under these conditions, the silica particles and the precipitated iron(III) entities must be positively charged, which prevents the heterocoagulation between both phases. At this pH value, surface precipitation is also unfavoured since the iron(III) species formed at the early stages of hydrolysis are also positively charged [17]. However, the attachment of the precipitated iron oxide particles to the silica surface would be allowed at the pH resulting for the $Fe(acac)_3$ solutions since it was (~ 6) between those of the two phases. In this case, the surface precipitation of the iron hydroxous-oxide could also take place through the condensation between the surface silanols and the uncharged species resulting from the hydrolysis of $Fe(acac)_3$, as schematized in Fig. 3a.

The addition of SDS to the $Fe(acac)_3$ starting dispersions had a positive effect on the coating process. Thus, the irregular particles precipitated in the absence of SDS progressively disappeared and the thickness of the coating increased as increasing the amount of SDS. In fact, only core shell parti-

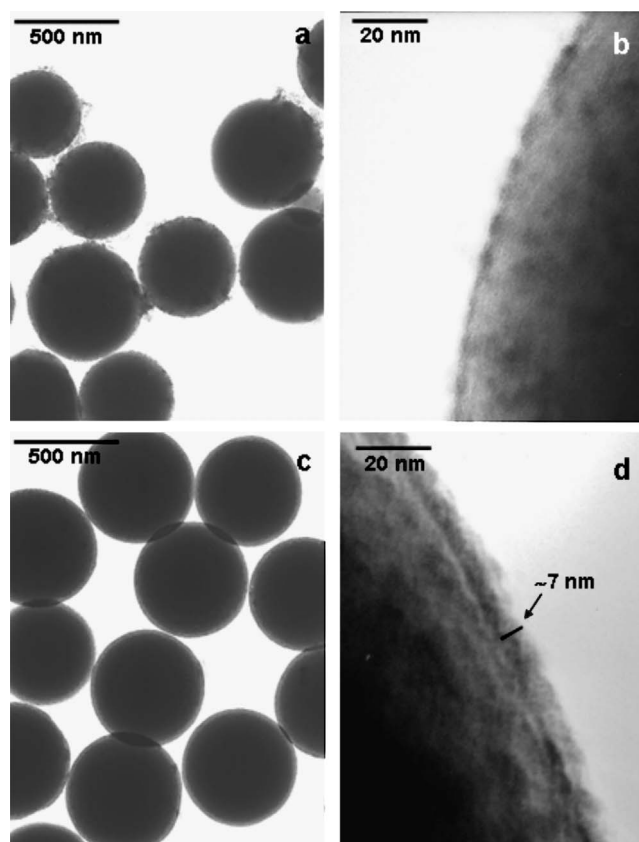


Fig. 1. TEM micrographs for the coated samples obtained from the $Fe(acac)_3$ solutions in the absence (a and b) or the presence (c and d) of SDS.

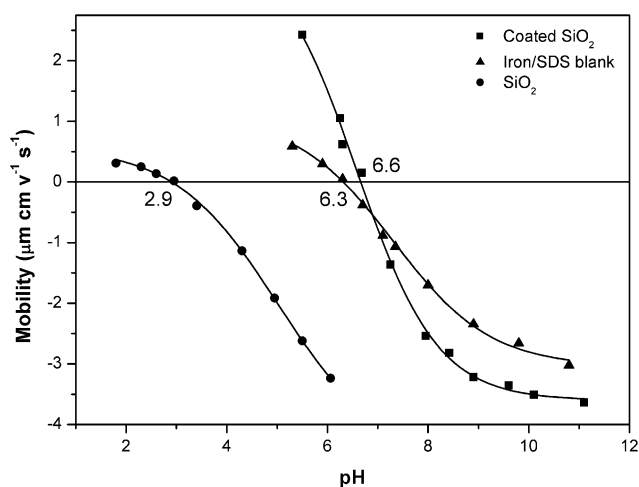


Fig. 2. Electrophoretic mobility measured as a function of pH for the coated sample obtained in the $Fe(acac)_3/SDS$ system, for the silica cores and for the iron oxide/SDS blank.

cles with smooth surface and a coating thickness of ~ 7 nm were detected for a $SDS/Fe(acac)_3$ mole ratio of 15 (Figs. 1c and 1d). The presence of iron in each single particle was confirmed by EDX analyses whereas the chemical analysis of this sample gave a Fe/Si atomic ratio similar (6.5%) to that resulting from the composition of the starting dispersion ($Fe/Si = 6.6\%$) suggesting the precipitation of most

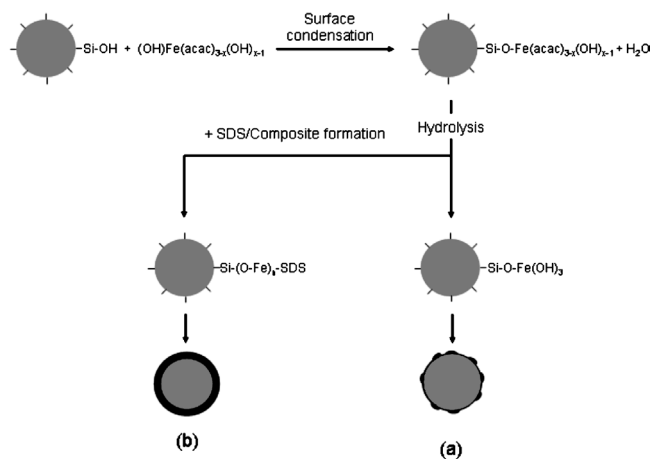


Fig. 3. Schematic representation of the mechanism of silica coating through surface precipitation from $\text{Fe}(\text{acac})_3$ solutions in the absence (a) or the presence (b) of SDS.

iron species. The effectiveness of this coating process was confirmed by the Fe/Si atomic ratio obtained from the Fe_{2p} and Si_{2p} XPS spectra measured for this sample, which was much higher (150%) than the value for the overall solid, indicating that the iron cations are mainly concentrated in the outermost layers of the silica spheres. In agreement with these observations, the iep of the coated particles was also much higher (6.6) than that of the cores (2.9) and very close to that of an iron oxide/SDS blank (6.3) precipitated under similar conditions but in the absence of silica (Fig. 2).

To explain the uniformity and smoothness of the coating obtained in the presence of SDS we must first address the nature for the iron compound precipitated in this case. It has been reported that when a SDS solution is mixed with aqueous solutions of iron(III) salts, layered iron oxide/surfactant composites are rapidly formed consisting of dodecylsulfate layers alternating with a few layers of iron oxide, the inorganic layer thickness depending on the extend of the hydrolysis-condensation reactions [18,19]. In these composites, the surfactant molecules are bounded to the iron oxide species through the sulfate groups whereas the stacking of these composite layers takes place by the mutual interpenetration of the hydrophobic tails of the surfactant molecules, which are arranged normal to the plane of the inorganic layer [18,19]. Although the formation of such iron oxide/SDS composites in the core-shell particles could not be detected either by IR absorption spectroscopy (the spectrum of the coated sample was dominated by the features of silica) or by XRD, probably due to the small coating thickness, it could be supported by the XRD pattern and the IR spectrum of the iron oxide/SDS blank. Thus, the XRD pattern (Fig. 4) of this solid consisted of weak and broad peaks at 2θ values (18° , 35.5° , 40.5° , 55° , 58.5° , and 62.5°) close to those expected for $\text{Fe}(\text{OH})_3$ [20], which would correspond to the inorganic part of the composite whereas its IR spectrum displayed bands in the $3100\text{--}2800$ and $1350\text{--}1150\text{ cm}^{-1}$ regions similar to those observed for SDS (Fig. 5), manifesting that this solid contained C–H

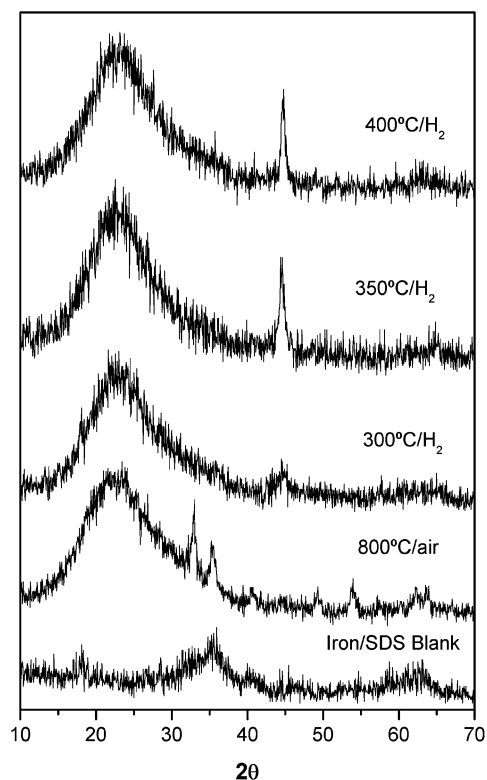


Fig. 4. X-ray diffraction patterns obtained for the coated sample obtained in the $\text{Fe}(\text{acac})_3/\text{SDS}$ system heated at different temperatures under air or hydrogen atmosphere and for the iron oxide/SDS blank.

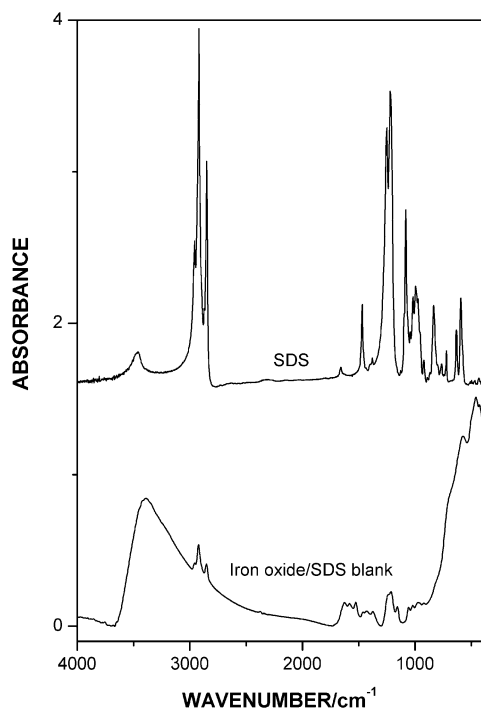


Fig. 5. Infrared spectra obtained for SDS and the iron oxide/SDS blank.

groups and sulfate anions, respectively [21]. Attempts to observe similar bands by DRIFTS spectroscopy in the coated sample were also carried out. However, the obtained spec-

trum only showed the presence of the C–H bands, whereas those corresponding to the sulfate groups could not be detected probably due to the overlapping with the strong Si–O band in the same frequency region ($\sim 1100\text{ cm}^{-1}$). In agreement with the formation of the iron oxide/SDS composite would also be the finding that the onset of precipitation took place much faster in the presence of SDS (around 1 min) than in its absence (about 3 h), since it has been reported that the precipitation of the iron oxide/SDS composites from the inorganic salts (nitrate and chloride) solutions is very fast even at low temperature ($40\text{ }^\circ\text{C}$) [18].

If the formation of an iron/SDS composite is then assumed, the uniform coating should result from the surface precipitation of this composite on the silica particles through the iron(III) species formed by hydrolysis of $\text{Fe}(\text{acac})_3$, as shown in Fig. 3b. It should be noted that the direct adhesion of these composites to the silica surface through the SDS chains must be discarded since as it has been reported, this anionic surfactant does not adsorb on the negatively charged hydrophilic surface of silica at the pH of our experiment (~ 6) [22].

Several experiments were also carried out in order to increase the thickness of the coating layer either by increasing the $\text{Fe}(\text{acac})_3$ concentration ($0.0034\text{ mol dm}^{-3}$) or by decreasing the amount of cores (1 g dm^{-3}) keeping constant the other experimental conditions. In effect, thicker coatings were obtained; however, the coated particles appeared bounded through their shells in all cases.

3.2. Thermal treatment and reduction of the core-shell particles

The thermal evolution of the coated particles was followed by X-ray diffraction (Fig. 4) up to the crystallization of the shell, which took place at $800\text{ }^\circ\text{C}$ either in air or inert (nitrogen) atmosphere, giving hematite ($\alpha\text{-Fe}_2\text{O}_3$) as the only crystalline phase [23]. After this treatment, an uniform coating was still observed on the silica cores, which retained their spherical shape (Fig. 6). It should be noted that this temperature of hematite crystallization is higher than that observed for the iron oxide/SDS blank ($500\text{ }^\circ\text{C}$) (data not shown) and those reported for the transformation of most iron hydrous oxides to hematite ($\leq 500\text{ }^\circ\text{C}$) [24], which may be due to the presence of SDS in the shell phase and/or its interaction with the silica surface.

The as-prepared core-shell particles were also thermally treated under hydrogen flow aiming to obtain magnetic composites. The X-ray diffraction patterns obtained after reduction at different temperatures are shown in Fig. 4. As observed, the most intense peak ($2\theta = 44.7^\circ$) corresponding to $\alpha\text{-Fe}$ was detected in all reduced samples along with the broad feature at 2θ between 15° and 30° due to amorphous silica, irrespective of the temperature of treatment. As expected, a narrowing of the $\alpha\text{-Fe}$ peak was observed as increasing the reduction temperature indicating an increase of the crystallite size (Fig. 6).

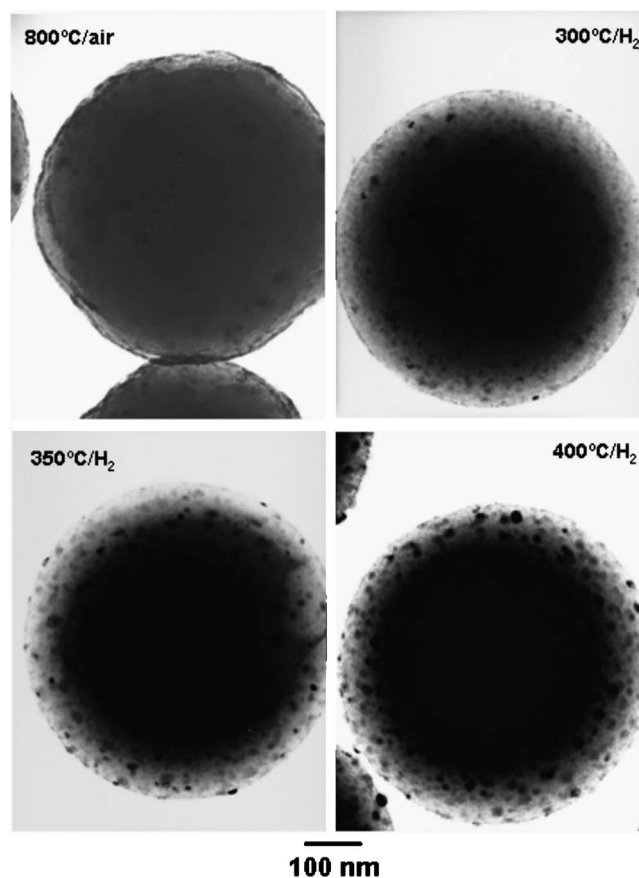


Fig. 6. TEM micrographs for the coated sample obtained in the $\text{Fe}(\text{acac})_3/\text{SDS}$ system heated at different temperatures under air or hydrogen atmosphere.

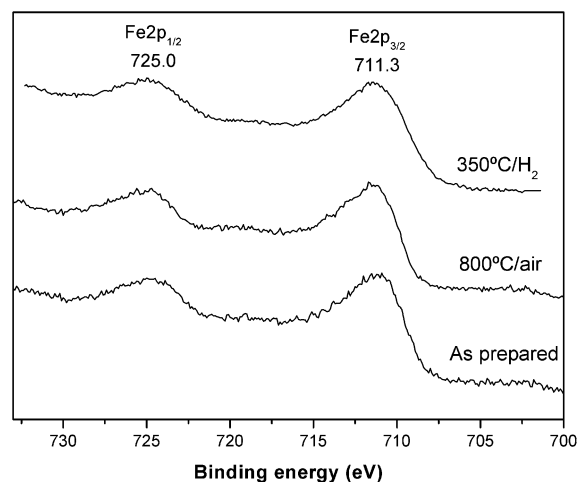


Fig. 7. Fe_{2p} XPS spectra for the coated sample obtained in the $\text{Fe}(\text{acac})_3/\text{SDS}$ system, as prepared and after heating at different temperatures under air or hydrogen atmosphere.

It should be noted that as illustrated in Fig. 7 for the sample reduced at $350\text{ }^\circ\text{C}$, the position of the Fe_{2p} bands (725 and 711.3 eV) observed in the XPS spectra of the reduced samples was similar to that corresponding to the original and the air annealed samples and therefore it was consis-

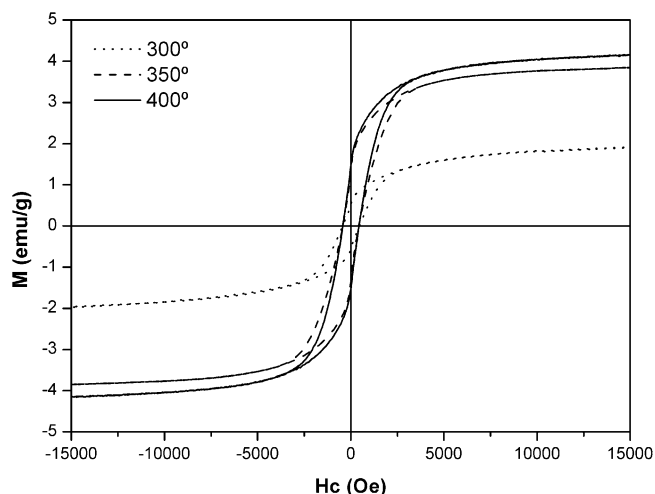


Fig. 8. Magnetization curves measured at room temperature for the iron/silica composite particles obtained using different reduction temperatures.

Table 1

Coercivity (H_c), saturation magnetization (M_s), remanent magnetization (M_r), and squareness (M_r/M_s) for the core-shell particles reduced at different temperatures

Temperature ($^{\circ}\text{C}$)	H_c (Oe)	M_s (emu g^{-1})	M_r (emu g^{-1})	M_r/M_s
300	447	2.0	0.52	0.26
350	420	4.0	1.40	0.35
400	430	4.2	1.44	0.34

tent with the presence of oxidized iron in the outer layers of the particles [25]. This iron oxide layer must be very thin and also of amorphous nature thus explaining why it is not observed in the XRD pattern of the sample (Fig. 4). This behaviour suggests an incomplete reduction or a partial reoxidation of the formed Fe crystallites when exposed to the air atmosphere. The analysis of the XPS data also showed that the Fe/Si atomic ratio obtained from the Fe_{2p} and Si_{2p} spectra for the reduced sample decreased (80%) with respect to that obtained for the as prepared coated particles (150%). According to the TEM observations (Fig. 6), such a behaviour could be explained by the rearrangement of the shell produced during reduction, which after this treatment appeared composed by individual iron-containing nanocrystallites rather than by a continuous coating.

The magnetic properties obtained from the hysteresis loops measured for the reduced samples (Fig. 8) are shown in Table 1. As observed, the saturation magnetization (M_s) of the sample reduced at 300°C was much lower (2 emu g^{-1}) than the theoretical value calculated assuming that the shell consists of pure iron (12.2 emu g^{-1}), taking into account the Fe/Si atomic ratio of the sample and a M_s value of 220 emu g^{-1} for iron [26]. This behaviour indicates that an important part of the iron crystallites was oxidized, which could be due at least in part to an incomplete reduction in agreement with the increase of M_s (4 emu g^{-1}) observed as increasing the reduction temperature up to 350°C . It should be noted that this M_s value, which was still lower than the

theoretical one, could not be significantly increased on a further temperature increase up to 400°C suggesting that the remaining iron oxide, also detected by XPS (Fig. 7), might result from a partial reoxidation of the iron crystallites in the air atmosphere rather than from an incomplete reduction. This oxidation process usually results in the formation of a passivation iron oxide layer as it has been previously detected for acicular iron nanoparticles [27]. By taking into consideration the theoretical M_s value above mentioned (12.2 emu g^{-1}) and a value of $10\text{--}20 \text{ emu g}^{-1}$ for the iron oxide layer (assumed to be nanocrystals of maghemite of about 2 nm) [28,29] we can approximately estimate the amount of oxidized iron, which correspond to an iron oxide/total iron mole fraction of about 90% for the sample reduced at 300°C and about 55% for the samples reduced at $350\text{--}400^{\circ}\text{C}$. Obviously, a more precise determination of the relative amount of both iron-containing species would require the examination of the samples by Mössbauer spectroscopy.

The values of H_c were less affected by the reduction temperature (Table 1). In fact, the observed changes are within the experimental error. These H_c values were similar to the theoretical value expected for noninteracting single-domain spherical iron particles oriented at random [30]. This magnetic behaviour is also suggested by the diameter of the iron crystallites (measured on the TEM micrographs), which was lower ($\sim 20 \text{ nm}$) than the critical diameter for monodomain spherical iron particles ($\sim 26 \text{ nm}$) [30].

Finally, it should be noted that the M_r/M_s values measured for these samples (<0.4) were significantly lower than the theoretical value expected for an assembly of spherical single-domain and noninteracting particles with cubic crystal anisotropy (three $\langle 100 \rangle$ easy axes) randomly oriented (0.83) [26]. Since the iron grains present monodomain character, this finding would indicate that either the iron oxide layer or a fraction of the smaller iron crystallites or both are superparamagnetic at room temperature [31]. The much lower M_r/M_s value obtained for the sample reduced at 300°C , which contained finer iron crystals (Fig. 6) and a higher amount of oxidized iron, would be in agreement with such an interpretation.

4. Conclusions

The aging at 85°C for 24 h of iron(III) acetylacetonate solutions in water/ethanol mixtures, containing sodium dodecylsulfate (SDS) and silica spheres (590 nm) resulted in core-shell particles composed by a silica core coated with a smooth layer, which seems to consist of a lamellar iron oxide/SDS composite. On heating at 800°C , this composite transforms into hematite keeping the layer uniformity. The thermal reduction under a hydrogen stream of the core-shell particles yielded magnetic composites consisting of rather uniform nanocrystallites ($\sim 20 \text{ nm}$) of partially oxidized iron homogeneously deposited on the silica particles. The satu-

ration magnetization and the squareness of these materials could be modified by changing the reduction temperature (from 300 to 400 °C), whereas their coercivity was less affected by this parameter. Most iron nanocrystallites present a ferromagnetic character although a small fraction, which increased as decreasing temperature, may behave as superparamagnetic at room temperature. The oxidized iron phase seems to be also superparamagnetic, irrespective of the reduction temperature.

Acknowledgments

This work was supported by the Spanish CICYT under projects MAT2002-04001-C02 and MAT2003-01479. The fellowship of R. Pozas from the Spanish Ministerio de Ciencia y Tecnología is gratefully acknowledged. Valuable suggestions by Dr. M.P. Morales are also acknowledged.

References

- [1] E. Matijević, *Langmuir* 10 (1994) 8.
- [2] F. Caruso, *Adv. Mater.* 13 (2001) 11.
- [3] M.C. Rangel, F. Galembeck, *J. Catal.* 145 (1994) 364.
- [4] M. Nath, B.C. Satishkumar, A. Govindaraj, C.P. Vinod, C.N.R. Rao, *Chem. Phys. Lett.* 322 (2000) 333.
- [5] P. Tartaj, M.P. Morales, S. Veintemillas-Verdaguer, T. González-Carreño, C.J. Serna, *J. Phys. D Appl. Phys.* 36 (2003) R182.
- [6] B. Ben-Nissan, *MRS Bull., Jan.* (2004) 28.
- [7] F. Caruso, A.S. Susa, M. Giersig, H. Möhwald, *Adv. Mater.* 11 (1999) 950.
- [8] H. Shiho, N. Kawahashi, *J. Colloid Interface Sci.* 226 (2000) 91.
- [9] P. Tartaj, *Chem. Phys. Chem.* 4 (2003) 1371.
- [10] W. Stöber, A. Fink, E. Bohn, *J. Colloid Interface Sci.* 26 (1968) 62.
- [11] M. Ohmori, E. Matijević, *J. Colloid Interface Sci.* 150 (1992) 594.
- [12] A.P. Philipse, M.P.B. Van Bruggenand, C. Pathmamanoharan, *Langmuir* 10 (1994) 92.
- [13] S. Ramesh, I. Felner, Y. Koltipin, A. Gedanken, *J. Mater. Res.* 15 (2000) 944.
- [14] Y. Zhu, H. Da, X. Yang, Y. Hu, *Colloids Surf. A Physicochem. Eng. Aspects* 231 (2003) 123.
- [15] M. Ocaña, A. González-Elipe, *Colloids Surf. A Physicochem. Eng. Aspects* 157 (1999) 315.
- [16] M. Kosmulski, E. Maczka, E. Jartych, J.B. Rosenholm, *Adv. Colloid Interface Sci.* 103 (2003) 57.
- [17] F. Burriel, S. Arribas, F. Lucena, J. Hernandez, *Qualitative Analytical Chemistry, Paraninfo, Madrid, Spain*, 1998, p. 586.
- [18] S.H. Tolbert, P. Sieger, G.D. Stucky, S.M.J. Aubin, C.C. Wu, D.N. Hendrickson, *J. Am. Chem. Soc.* 119 (1997) 8652.
- [19] G. Wirmsberger, K. Gatterer, P. Behrens, *J. Mater. Chem.* 8 (1998) 1509.
- [20] JCPDF File No. 22-346.
- [21] N.B. Colthup, L.H. Daly, S.E. Wiberley, *Introduction to Infrared and Raman Spectroscopy*, Academic Press, San Diego, 1990.
- [22] J. Penfold, E. Staples, I. Tucker, R.K. Thomas, *Langmuir* 18 (2002) 5755.
- [23] JCPDF File No. 33-664.
- [24] R.M. Cornell, U. Schwertmann, *The Iron Oxides. Structure, Properties, Reactions, Occurrence and Uses*, VCH-Weinheim, Germany, 1996, p. 171.
- [25] C.D. Wagner, W.H. Riggs, L.E. Davis, J.F. Moulder, G.E. Muilenberg, *Handbook of X-Ray Photoelectron Spectroscopy*, Perkin-Elmer Corporation, Minnesota, 1973, p. 81.
- [26] B.D. Cullity, *Introduction to Magnetic Materials*, Addison-Wesley, Reading, MA, 1972.
- [27] N.O. Nuñez, R. Pozas, M.P. Morales, P. Tartaj, P. Bonville, A.R. González-Elipe, A. Caballero, M. Ocaña, C.J. Serna, *Chem. Mater.* 15 (2003) 951.
- [28] M.P. Morales, S. Veintemillas-Verdaguer, M.I. Montero, C.J. Serna, A. Roig, Ll. Casas, B. Martínez, F. Sandiumenge, *Chem. Mater.* 11 (1999) 3058.
- [29] P. Tartaj, T. González-Carreño, C.J. Serna, *Adv. Mater.* 13 (2001) 1620.
- [30] H. Zijlstra, in: E.P. Wohlfarth (Ed.), *Ferromagnetic Materials*, vol. 3, North-Holland, Amsterdam, 1982, p. 56.
- [31] G. Bate, in: E.P. Wohlfarth (Ed.), *Recording Materials*, vol. 2, North-Holland, Amsterdam, 1980, p. 443.